Theoretical and Experimental Chemistry, Vol. 57, No. 2, May, 2021 (Ukrainian Original Vol. 57, No. 2, March-April, 2021)

INFLUENCE OF SOLVENT ON STABILITY AND ELECTROPHYSICAL PROPERTIES OF ORGANIC–INORGANIC PEROVSKITES FILMS $CH_3NH_3PBI_3$

P. V. Torchinyuk,[1] O. I. V'yunov,[1] L. L. Kovalenko,[1] A. A. Ischenko,[2] I. V. Kurdyukova,[2] and A. G. Belous[1]

UDC 544.032.732:539.216

The influence of DMF and DMSO solvents on the properties of organic–inorganic perovskite films obtained at the ratio of starting reagents PbI_2:CH_3NH_3I = 1:2 was studied. It was found that a thicker film is formed from solutions in DMSO. XRD and fluorescence spectroscopy have shown that the use of DMSO promotes the formation of perovskite films that are less sensitive to moisture and irradiation. It is shown that the mobility of charge carriers in perovskite films obtained from DMSO ($\mu = 67 \pm 5$ $cm^2/V{\cdot}s$) is an order of magnitude higher than for the films obtained from DMF ($\mu = 9.1 \pm 0.7$ $cm^2/V{\cdot}s$). The density of charge carriers is $n = (3.8 \pm 0.3){\cdot}10^{19}$ cm^{-3} and $n = (2.9 \pm 0.2){\cdot}10^{19}$ cm^{-3} when using DMF and DMSO solvents, respectively. The formed organic–inorganic perovskite films with DMSO were found to have higher conductivity than films obtained from DMF.

Keywords: *organic–inorganic perovskite, microstructure, complex impedance, I–V curves, stability.*

The ABX_3 organic–inorganic perovskites (A = CH_3,NH_3^+, $HC(NH_2)_2^+$, B = Pb, Sn; X = I, Br, Cl) are photoactive materials that can be used to produce highly efficient solar cells that are not inferior in terms of energy conversion efficiency to traditional photovoltaic technologies [1-3]. This type of material was studied by Weber in 1978 for the first time [4, 5]. Currently, the solar energy conversion efficiency of the perovskite-based cells is 25.2% [6-10]. The high importance of the solar energy conversion efficiency also contributes to their integration with other electronic devices, such as supercapacitors [11, 12] and accumulator batteries [13, 14]. In addition, perovskite materials are also used as photodetectors [15], smart windows [16], and solar fuel [17].

The main obstacles to the large-scale use of organic–inorganic perovskite-based solar cells are the thermal and chemical instability of $CH_3NH_3PbI_3$ [18]. It is possible to replace the organic component of iodine with other halides (chlorine, bromine) in order to increase the stability of the cells [19]. The replacement of methylammonium ions with inorganic cations

[1]V. I. Vernadsky Institute of General and Inorganic Chemistry, NAS of Ukraine, Kyiv, Ukraine. E-mail: belous@ionc.kiev.ua.
[2]Institute of Organic Chemistry, NAS of Ukraine, Kyiv, Ukraine E-mail: al.al.ishchenko@gmail.com.

Translated from Teoretychna ta Eksperymentalna Khimiya, Vol. 57. No. 2. pp. 93-98, March-April, 2021. Original article submitted April 2, 2021; revised May 17, 2021.

(Cs, Rb) and introduction of other halides (bromide and chloride) improves the stability of $CH_3NH_3PbI_3$ perovskite, but such changes in its composition also cause changes in the width of the band gap in it.

Organic–inorganic perovskites can be easily synthesized by precipitation methods from solutions that are simple and reliable. These methods include one-step and two-step deposition, and it is possible to obtain high-quality organic–inorganic perovskite films using these methods [21]. The PbI_2 and methylammonium iodide MAI starting reagents are widely available for perovskite synthesis and are soluble in organic solvents, mainly dimethyl sulfoxide (DMSO), dimethylformamide (DMF), γ-butyrolactone (GBL), and acetonitrile (ACN).

Studies of volt-ampere characteristics (VAC) of organic–inorganic perovskites were performed on single crystals [22] and polycrystalline samples [23]. The work [22] used $MAPbI_3$ single crystals to study the *I–V* dependences, which were synthesized at a ratio of starting reagents PbI_2:CH_3NH_3I = 1:3 in a GBL solvent using the antisolvent method (dichloromethane was used as an antisolvent). The study of *I–V* dependences was performed by the four-probe method using two types of contacts: contact with Ti and contact with MoO_3/Au/Ag. The work [23] developed a method for measuring the VAC for polycrystalline samples of organic–inorganic perovskites for the first time and studied the volt-ampere characteristics of a polycrystalline film of organic–inorganic perovskites. It should be noted that perovskite films were obtained at different ratios of PbI_2 and CH_3NH_3I starting reagents (1:1, 1:2, 1:3) using DMF solvent. The best *I–V* characteristics, such as the conductivity, is demonstrated by a film obtained at a 1:2 ratio of starting reagents when using a DMF solvent.

The aim of this work was to study the effect of DMF and DMSO solvents on the stability and electrical properties (volt-ampere characteristics) of organic–inorganic perovskite films obtained at a ratio of starting reagents PbI_2 and CH_3NH_3I of 1:2.

EXPERIMENTAL

Lead iodide (PbI_2) and methylammonium iodide (CH_3NH_3I) were used as starting reagents for the $CH_3NH_3PbI_3$ perovskite synthesis. Iodine was partially replaced by chlorine in all the studied samples in order to stabilize the perovskite structure; therefore, methylammonium chloride CH_3NH_3Cl (chemically pure) was added. [24]. The solvent was dried DMSO (chemically pure) and DMF (chemically pure).

Solutions with PbI_2 and CH_3NH_3I reagents were preliminarily prepared in DMSO and DMF solvents in a 1:2 ratio in order to obtain $CH_3NH_3PbI_3$ films. The above solutions were stirred at a temperature of 70°C for 1 h in order to completely dissolve the reagents. The formation of $CH_3NH_3PbI_3$ crystalline films was performed in a dry box. The previously obtained clear solution was deposited on cleaned glass supporters by spin-coating at a speed of 1200 rpm for 30 s. Heat treatment of the films was performed for 15 min in a preheated to 190°C oven.

The studies of the synthesized film microstructure based on $CH_3NH_3PbI_3$ perovskites obtained at different ratios of starting reagents were performed on a miniSEM SNE 4500MB scanning electron microscope (SEC). The surface degree of filling was calculated using the electron microscopy data in order to estimate the density of films; therefore, image binarization was performed, and an adequate threshold was determined to identify and correlate the area of the film to the total area [25].

The phase state of the synthesized perovskite films was characterized by the X-ray powder diffraction pattern recorded on a DRON-4-07 device (CuK_α radiation, 30 kV, 30 mA). The spectra were recorded in the angular range of 2θ from 5 to 70° with a step of 0.03°, and the exposure time was 3 s.

The kinetics of fluorescence was studied on a CM 2203 spectrofluorimeter (Belarus) under excitation by radiation with a wavelength of 470 nm in the absorption band of perovskite; at the same time, the fluorescence intensity was recorded in the region of its maximum radiation (780 nm). The study was performed in a dry (humidity ≤7 ppm) atmosphere, which was obtained by drying the balloon nitrogen.

The $Z = Z' + iZ''$ complex impedance measurements (where Z' and Z'' are real and imaginary parts of complex impedance) were performed on a 1260A Impedance/Gain-Phase Analyzer (Solartron Analytical) in a wide frequency range (1 Hz–1 MHz) with increasing voltage from 0 to 40 V. The voltage measurement error was ±(10 mV + 1%). A multilayer system was created for the measurement, which consisted of a supporter on which Au electrodes and perovskite films were deposited (Fig. 1).

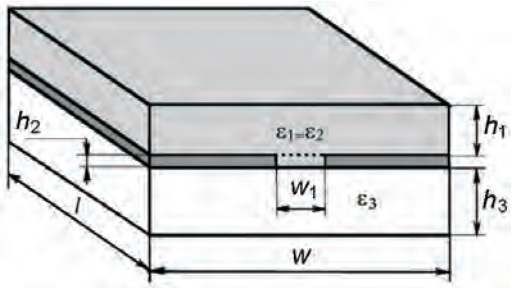

Fig. 1. Scheme of the measured multilayer system consisting of a glass supporter (w = 16 mm, l = 24 mm, h_3 = 1 mm) on which Au electrodes with a thickness of h_2 = 90 nm were deposited at a distance of w_1 = 250 ± 4 m. The thickness of the studied film was h_1 = 500 nm.

The equivalent circuit and the values of its components were determined using ZView® program for Windows (Scribner Associates Inc., USA). The capacitance determining error was 1.5%. The complex impedance measurements were performed on the day of synthesis in a dry (humidity ≤7 ppm) atmosphere, which was obtained by drying balloon nitrogen in order to prevent film degradation and changes in the perovskite microstructure and properties [26]. The studies were performed in the dark and with light of 10 mW/cm^2 (corresponding to 0.1 sunlight at noon at the equator). An Infolight H3 lamp xenon lamp (Akodgy, Seoul, South Korea) with a power of 50 W was used as a light source. The light intensity was measured using a Lux/FC Light Meter DL-204. The volt-ampere characteristics of the films were calculated from the obtained data. The errors of indirect measurements were calculated for the functional parameters of the films, which were 8% for the mobility and density of charge carriers.

RESULTS AND DISCUSSION

Microstructure of organic–inorganic perovskite. Figure 2 shows the surface image of the synthesized films obtained on glass supporters at a ratio of starting reagents PbI_2 and CH_3NH_3I of 1:2 in DMF and DMSO solvents. According to the images, the morphology of the synthesized films is similar and is represented by particles in the form of a leaf. However, the film obtained using a DMSO solvent has a higher density: its surface degree of filling reaches 0.90, while it is equal to 0.84 when using a DMF solvent.

The impedance curves for organic–inorganic perovskite films obtained at a 1:2 ratio of starting reagents in DMF and DMSO solvents are typical curves for materials with electronic conductivity (Fig. 3). Figure 3 shows one semicircle for each sample in the complex impedance diagram, which is described by an equivalent circuit consisting of capacitors and film resistance connected in parallel [27]. The parameters of the conductive parts and the supporter were determined by measuring the cell on which the film was not deposited. These parameters were considered in the analysis of the circuit.

The partial capacitance method was used to determine the dielectric constant and current density for $CH_3NH_3PbI_3$ perovskite films obtained with different solvents [28]. The essence of this method is to represent a multilayer system in the form of three flat capacitors C_1, C_2, and C_3 connected in parallel, which are characterized by a homogeneous filling. The capacitance of the C system was determined as the sum of three partial capacitances $C = C_1 + C_2 + C_3$, where C_1, C_2, and C_3 are the capacitances of the components of the flat capacitor: the outer rectangular part of the film (1), the inner rectangular part of the film (2), and the supporter (3). The $CH_3NH_3PbI_3$ perovskite film was conventionally divided into an inner rectangular part with width w and thickness h_1 and an outer rectangular part with width w_1 and thickness h_2 to determine the capacitance of the system.

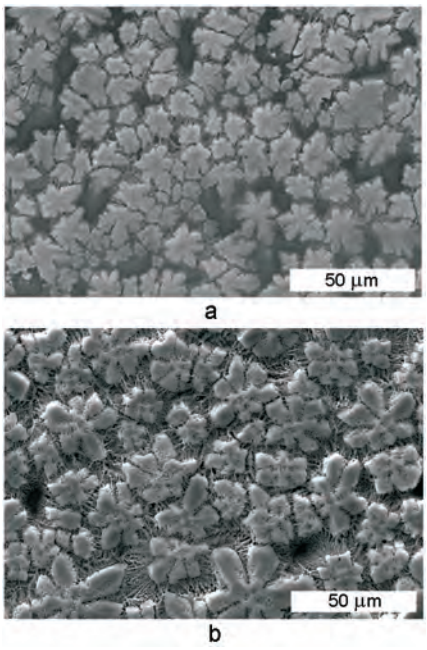

Fig. 2. Image of the surface of synthesized films based on $CH_3NH_3PbI_3$ perovskite obtained at a ratio of starting reagents PbI_2 and CH_3NH_3I of 1:2 in DMF (a) and DMSO (b) solvents.

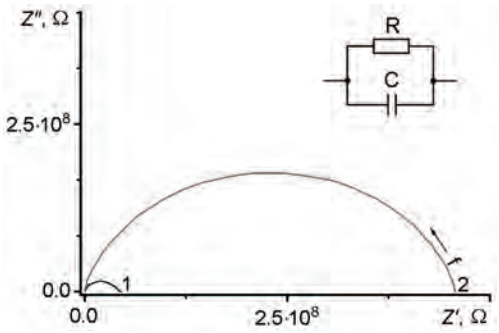

Fig. 3. Complex impedance diagrams in Nyquist coordinates and equivalent circuit of a multilayer system consisting of a glass supporter and an organic–inorganic perovskite film, which was obtained at a ratio of starting reagents (PbI_2 and CH_3NH_3I of 1:2 in DMSO (1) and DMF (2) solvent at an illumination of 10 mW/cm^2. The measurements were performed at a voltage of 1.7 V in a dry atmosphere.

The equation of a flat capacitor $C_2 = \varepsilon\varepsilon_0 A$, where $A = lh_2/w_1$, was used to determine the capacitance of the inner part of the film. The capacitance of the outer part of the film and the supporter was determined using conformal mappings based on the Schwarz–Christoffel transformation, adapted in Gevorgyan's approach [29]. According to this method, the elliptical

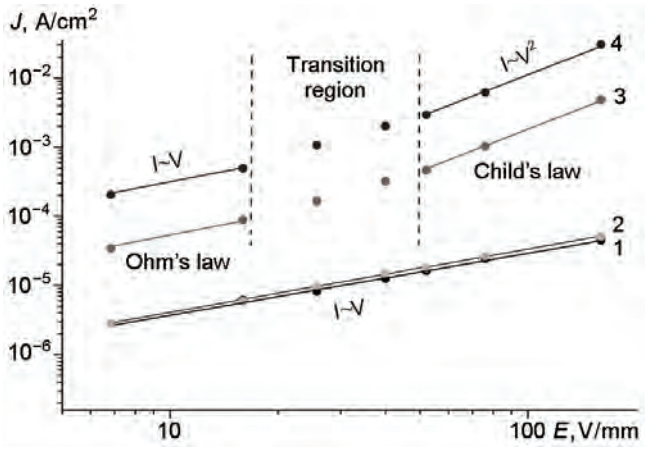

Fig. 4. Dependence of current density on the field strength for organic–inorganic perovskites obtained at a 1:2 ratio of starting reagents (PbI_2 and CH_3NH_3I) in DMF (1, 3) and DMSO (2, 4) solvents at different light intensity levels, 0 (1, 2) and 10 mW/cm^2 (3, 4).

distribution of electric fields in the sample is conventionally converted into a rectangle. In this case, the capacitance of the supporter will be expressed by the formula $C_{1.3} = \varepsilon_{1.3}\varepsilon_0 B$, where $B = K(k')/2K(k)$ and $k' = \sqrt{1-k^2}$; $K(k)$ is a complete elliptic integral of the first kind; k is the modulus of the elliptic integral; ε_0 is the dielectric constant of vacuum; ε_r is the dielectric constant of the supporter. The approximation proposed in the study [30] was used to solve elliptic integrals. The value of the dielectric constant of the insulating glass supporter for electrical applications (e-glass) is known and amounts to $\varepsilon = 6.6$ [31]; therefore, only the dielectric constant of the organic–inorganic perovskite remains unknown in the equations. Assuming that different regions of the perovskite film have the same value of dielectric constant, its formula is obtained in the form $\varepsilon_1 = C - \varepsilon_3\varepsilon_0 B/\varepsilon_0(A + B)$. This equation was used to calculate the dielectric constant of organic–inorganic perovskites.

The dielectric constant of the material was calculated for organic–inorganic perovskite films obtained using DMF and DMSO solvents. The experimental values of dielectric constant for perovskite films obtained at a 1:2 ratio of starting reagents using DMF and DMSO are $\varepsilon = 52$ and $\varepsilon = 44$, respectively.

A similar approach was used to determine the current density, such as the current of the multilayer system, which at a certain voltage was determined by Ohm's law and was defined as the sum of three partial currents: $I = I_1 + I_2 + I_3$, where I_1, I_2, I_3 are the currents of the components of the studied multilayer system: the outer rectangular part of the film (1), the inner rectangular part of the film (2), and the supporter (3). Since the distribution of current density values as well as the electric field strength is elliptical, the geometric factors were identical to those calculated for the capacitance values, such as $I_{1.3} = UB/$; $I_2 = UA/$. These equations connect the experimentally determined value of the current of the system as total I with the unknown value of the current flowing in the organic–inorganic perovskite film. Assuming that different regions of the perovskite film have the same value of resistivity, the following equation is obtained: $I_2 = A(I - UB/\ _3)/(A + B)$. Considering that the resistivity of glass is very high, the equation can be simplified: $I_2 = IA/(A + B)$.

Figure 4 shows the dependences of the current density on the voltage calculated from the impedance curves for organic–inorganic perovskites.

According to Fig. 4, the dark current depends linearly on the applied electric voltage (curves 1 and 2); at the same time there are several areas at illumination (curves 3 and 4).

There are three sites of volt-ampere dependences for organic–inorganic perovskites films: the VAC is described by Ohm's law ($I \sim V$) at low voltages and by Child's law ($I \sim V^2$) at increased voltages; at the same time, a transition region is present. These regions are also present for single-crystal organic–inorganic perovskites [22].

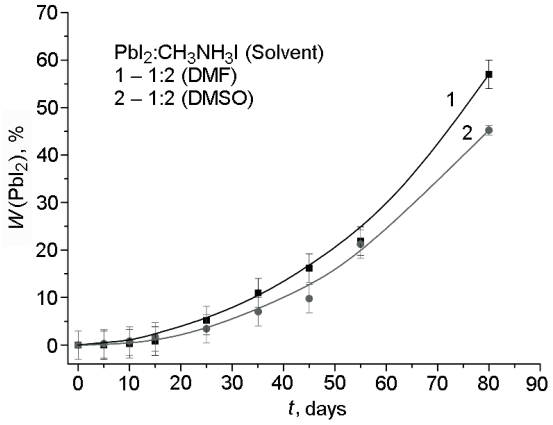

Fig. 5. Dependence of the content of the PbI_2 phase formed during the decomposition of perovskites obtained from a DMF (1) and DMSO (2) solution.

A linear VAC is observed in the absence of illumination, which is described by Ohm's law. The linear VAC dependence may be due to the fact that the organic–inorganic perovskite film may contain traps for charge carriers. A trapless mode is observed (traps do not hold charge carriers) when illuminating perovskite films, and the dependence is described by Child's quadratic law at high voltages and illumination (Fig. 4).

It is possible to perform calculations for the density and mobility of charge carriers using these regions and transitions between them [32]. The dependence of current (I) on the electric field voltage (V) in the Child's region is used to determine the mobility of charge carriers, which is determined by the equation $j = (9/8)\varepsilon\varepsilon_0 \ V^2/w_1^3$ (where ε is the dielectric constant of the sample, is the mobility, and w_1 is the distance between the electrodes). The mobility of charge carriers at a voltage of 40 V in the organic–inorganic perovskite film obtained using DMF solvent is $= 9.1 \pm 0.7$ cm^2/V·s, while $= 67 \pm 5$ cm^2/V·s using DMSO. Therefore, the mobility of charge carriers in the perovskite films obtained at a 1:2 ratio in DMSO is an order of magnitude higher than for films obtained using DMF solvent.

The dependence of current on the electric field voltage in the ohmic region is used to determine the density of charge carriers, which is described by the equation $j = e \ nV/w_1$ (n is the density of charge carriers and is the mobility determined in the Child's region). The density of charge carriers n in the ohmic region at a voltage of 4 V in the organic–inorganic perovskite film obtained using a DMF solvent is $n = (3.8 \pm 0.3)\cdot10^{19}$ m^{-3}, and $n = (2.9 \pm 0.2)\cdot10^{19}$ m^{-3} using DMSO.

Figure 4 shows that the organic–inorganic film obtained at a 1:2 ratio of the starting components in the DMSO solvent has a higher conductivity than the film obtained from the DMF solvent. At the same time, the almost similar slope in the ohmic region at the same level of illumination indicates the same level of charge carrier generation.

Study of film stability. The resistance of organic–inorganic perovskite films obtained at a 1:2 ratio of starting reagents in DMF and DMSO solvents to the action of moisture and irradiation was studied. It is known that organic–inorganic perovskites decompose into PbI_2 and other components under the influence of external factors. The resistance of organic–inorganic perovskites to the action of moisture was studied by XRD. The effect of irradiation on the stability of perovskites was determined by fluorescence spectroscopy.

According to the obtained XRD data, we plot the dependence of the content of the PbI_2 phase, which is formed as a result of degradation of the organic–inorganic perovskite film, on the exposure time to moisture (Fig. 5). The $CH_3NH_3PbI_3$ organic–inorganic perovskite films, obtained from solutions with a 1:2 ratio of starting reagents in DMF and DMSO solvents, show different resistance to moisture. The perovskite films obtained from DMSO solution are more resistant to moisture than the films obtained from DMF solution (Fig. 5, curves 1, 2).

There are changes in the fluorescence intensity over time when irradiating the perovskite films obtained from DMF and DMSO solutions. The fluorescence intensity increases over time (Fig. 6, curve 1) when irradiating the perovskite films

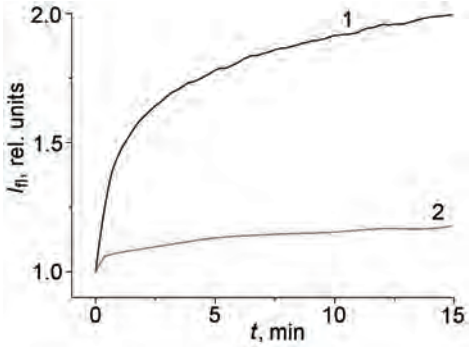

Fig. 6. Dependence of the I_{fl} fluorescence intensity of organic–inorganic perovskite films obtained from DMF (1) and DMSO (2) solutions with a 1:2 ratio of starting reagents on the exposure time in a dry atmosphere.

obtained from DMF solution, which is probably due to the subsequent change in the morphology of the film. The fluorescence intensity of the films obtained from DMSO solution does not change (Fig. 6, curve 2) under similar conditions, which indicates their much higher resistance to irradiation.

Therefore, the microstructure of the organic–inorganic perovskite films obtained at the ratio of starting reagents PbI_2: CH_3NH_3I = 1:2 in DMF and DMSO solvents was studied. It is shown that the microstructure of the films is similar and is represented by particles in the form of leaves. The use of DMSO solvent promotes the formation of a denser film. The electrical properties of perovskites were studied by impedance spectroscopy. It was found that the mobility of charge carriers in the perovskite films obtained at a 1:2 ratio in DMSO (= 67 ± 5 $cm^2/V·s$) is an order of magnitude higher than for the films obtained using a DMF solvent (= 9.1 ± 0.7 $cm^2/V·s$), which is associated with the formation of a denser perovskite film obtained from DMSO solvent. The density of charge carriers for the perovskites obtained from DMSO is $n = (2.9 \pm 0.2)·10^{19}$ cm^{-3} and is slightly less than for the perovskite films obtained from DMF, $n = (3.8 \pm 0.3)·10^{19}$ cm^{-3}. It was found that the organic–inorganic perovskite film obtained using DMSO has a higher conductivity than the film obtained using DMF solvent.

According to the XRD and fluorescence spectroscopy data, the resistance of organic–inorganic perovskite films obtained at the ratio of starting reagents PbI_2:CN_3NH_3I = 1:2 to the action of moisture and irradiation increases when replacing DMF with DMSO in the synthesis.

REFERENCES

1. M. A. Green, A. Ho-Baillie, and H. J. Snaith, *Nat. Photonics*, **8,** 506-514 (2014), doi: 10.1038/nphoton.2014.134.
2. S. A. Olaleru, J. K. Kirui, D. Wamwangi, et al., *Sol. Energy*, **196,** 295-309 (2020), doi: 10.1016/j.solener.2019.12.025.
3. A. G. Belous, A. A. Ishchenko, O. I. V'yunov, and P. V. Torchyniuk, *Theor. Exp. Chem*., **56,** 359-386 (2021), doi: 10.1007/s11237-021-09666-6.
4. D. Weber, *Z. Naturforsch*., **33b,** 1443-1445 (1978).
5. D. Weber, *Z. Naturforsch*., **33b,** 862-865 (1978).
6. J. Burschka, N. Pellet, S.-J. Moon, et al., *Nature*, **499,** 316-319 (2013), doi: 10.1038/nature12340.
7. M. Saliba, T. Matsui, K. Domanski, et al., *Science*, **354,** 206-209 (2016), doi: 10.1126/science.aah5557.
8. Q. Jiang, Y. Zhao, X. Zhang, et al., *Nat. Photonics*, **13,** 460-466 (2019), doi: 10.1038/s41566-019-0398-2.
9. H. Min, M. Kim, S.-U. Lee, et al., *Science*, **366,** 749-753 (2019), doi: 10.1126/science.aay7044.
10. Best Research-Cell Efficiency Chart., URL: (accessed 24 March, 2021) (2021)
11. X. Xu, S. Li, H. Zhang, et al., *ACS Nano*, **9,** 1782-1787 (2015), doi: 10.1021/nn506651m.

12. J. Liang, G. Zhu, Z. Lu, et al., *J. Mater. Chem. A*, **6,** 2047-2052 (2018), doi: 10.1039/c7ta09099d.
13. Q. Wang, H. Chen, E. McFarland, et al., *Adv. Energy Mater*., **5,** 1501418 (2015), doi: 10.1002/aenm.201501418.
14. A. Gurung, K. Chen, R. Khan, et al., *Adv. Energy Mater*., **7,** 1602105 (2017), doi: 10.1002/aenm.201602105.
15. P. Ramasamy, D.-H. Lim, B. Kim, et al., *Chem. Commun*., **52,** 2067-2070 (2016), doi: 10.1039/C5CC08643D.
16. X. Xia, Z. Ku, D. Zhou, et al., *Mater. Horizons*, **3,** 588-595 (2016), doi: 10.1039/C6MH00159A.
17. P. V. Kamat, *ACS Energy Lett*., **3,** 28-29 (2018), doi: 10.1021/acsenergylett.7b01134.
18. A. F. Akbulatov, S. Y. Luchkin, L. A. Frolova, et al., *J. Phys. Chem. Lett*., **8,** 1211-1218 (2017), doi: 10.1021/acs.jpclett.6b03026.
19. E. L. Unger, A. R. Bowring, C. J. Tassone, et al., *Chem. Mater*., **26,** 7158-7165 (2014), doi:10.1021/cm503828b.
20. F. Sani, S. Shafie, H. N. Lim, et al., *Materials*, **11,** 1008 (2018), doi: 10.3390/ma11061008.
21. N. K. Noel, S. N. Habisreutinger, B. Wenger, et al., *Energy Environ. Sci*., **10,** 145-152 (2017), doi: 10.1039/C6EE02373H.
22. V. Adinolfi, M. Yuan, R. Comin, et al., *Adv. Mater*., **28,** 3406-3410 (2016), doi: 10.1002/adma.201505162.
23. O. I. V'yunov, A. G. Belous, S. D. Kobylianska, et al., *Nanoscale Res. Lett*., **13,** 98 (2018), doi: 10.1186/s11671-018-2509-2.
24. A. G. Belous, O. I. V'yunov, S. D. Kobylianska, et al., *Russ. J. Gen. Chem*., **88,** 114-119 (2018), doi: 10.1134/S1070363218010188.
25. E. M. Palmero, D. Casaleiz, J. de Vicente, et al., *Compos. Part A: Appl. Sci. Manuf*., **124,** 105497 (2019), doi: 10.1016/j.compositesa.2019.105497.
26. W. Huang, J. S. Manser, P. V. Kamat, et al., *Chem. Mater.*, **28,** 303-311 (2016), doi: 10.1021/acs.chemmater.5b04122.
27. A. Dualeh, T. Moehl, N. Tutreault, et al., *ACS Nano*, **8,** 362-373 (2013), doi: 10.1021/nn404323g.
28. O. G. Vendik, S. P. Zubko, and M. A. Nikolsky, *Zh. Tekh. Fiz.,* **69,** 1-7 (1999).
29. S. S. Gevorgian, T. Martinsson, P. L. J. Linner, et al., *IEEE Trans. Microwave Theory Tech.*, **44,** 896-904 (1996), doi: 10.1109/22.506449.
30. M. W. den Otter, *Sens. Actuator A: Phys.*, **96,** 140-144 (2002), doi: 10.1016/S0924-4247(01)00783-X.
31. Y. I. Kolesov, M. Y. Kudryavtsev, and N. Y. Mikhailenko, *Glass Ceram*., **58,** 197-202 (2001), doi: 10.1023/A:1012386814248.
32. W. Peng, X. Miao, V. Adinolfi, et al., *Angew. Chem. Int. Ed*., **55,** 10686-10690 (2016), doi: 10.1002/anie.201604880.